J Physiol 586.23 (2008) pp 5743–5755

The Journal of Physiology

Spontaneous purinergic neurotransmission in the mouse urinary bladder

John S. Young[1], En Meng[1,2], Tom C. Cunnane[1] and Keith L. Brain[1]

[1] *Department of Pharmacology, University of Oxford, Mansfield Road, Oxford OX1 3QT, UK*
[2] *Division of Urology, Department of Surgery, Tri-Service General Hospital, no. 325, Sec. 2, Chenggong Road, Neihu, Taipei 114, Taiwan, ROC*

Spontaneous purinergic neurotransmission was characterized in the mouse urinary bladder, a model for the pathological or ageing human bladder. Intracellular electrophysiological recording from smooth muscle cells of the detrusor muscle revealed spontaneous depolarizations, distinguishable from spontaneous action potentials (sAPs) by their amplitude (< 40 mV) and insensitivity to the L-type Ca^{2+} channel blocker nifedipine (1 μM) (100 ± 29%). Spontaneous depolarizations were abolished by the $P2X_1$ receptor antagonist NF449 (10 μM) (frequency 8.5 ± 8.5% of controls), insensitive to the muscarinic acetylcholine receptor antagonist atropine (1 μM) (103.4 ± 3.0%), and became more frequent in latrotoxin (LTX; 1 nM) (438 ± 95%), suggesting that they are spontaneous excitatory junction potentials (sEJPs). Such sEJPs were correlated, in amplitude and timing, with focal Ca^{2+} transients in smooth muscle cells (measured using confocal microscopy), suggesting a common origin: ATP binding to $P2X_1$ receptors. sAPs were abolished by NF449, insensitive to atropine (126 ± 39%) and increased in frequency by LTX (930 ± 450%) suggesting a neurogenic, purinergic origin, in common with sEJPs. By comparing the kinetics of sAPs and sEJPs, we demonstrated that sAPs occur when sufficient cation influx through $P2X_1$ receptors triggers L-type Ca^{2+} channels; the first peak of the differentiated rising phase of depolarizations – attributed to the influx of cations through the $P2X_1$ receptor – is of larger amplitude for sAPs (2248 mV s^{-1}) than sEJPs (439 mV s^{-1}). Surprisingly, sAPs in the mouse urinary bladder, unlike those from other species, are triggered by stochastic ATP release from parasympathetic nerve terminals rather than being myogenic.

(Received 21 August 2008; accepted after revision 12 October 2008; first published online 20 October 2008)
Corresponding author J. S. Young: Department of Pharmacology, University of Oxford, Mansfield Road, Oxford OX1 3QT, UK. Email: john.s.young@gmail.com

In most mammals, excitation of the detrusor muscle of the urinary bladder is achieved through the parasympathetic activation of both purinergic and cholinergic neurotransmission, leading to voiding of the bladder. The brief, initial phase of contraction is atropine insensitive (Henderson & Roepke, 1934) and purinergic (Burnstock *et al.* 1978); the second phase, of longer duration, is cholinergic (Krell *et al.* 1981). The balance between purinergic and cholinergic neurotransmission observed experimentally varies widely. This variation is often attributed to the following three factors. (i) *Species used*. Detrusor contraction is almost entirely controlled by purinergic neurotransmission in cat (Nergårdh, 1981) and rabbit (Sibley, 1984), whereas cholinergic neurotransmission dominates in the Old World primates (Craggs & Stephenson, 1985). (ii) *Age*. For example, there is an increase with age in the contribution of purinergic neurotransmission to bladder voiding in the human (Yoshida *et al.* 2001) and rat (Saito *et al.* 1991). (iii) *Experimental protocol*. Single pulse or low frequency, repetitive transmural electrical stimulation evokes an atropine-insensitive contraction (Ambache & Zar, 1970); high frequency repetitive stimulation evokes excitation that comprises a much larger proportion of cholinergic than purinergic neurotransmission (Sibley, 1984).

Normal voiding of the human bladder is attributed to the actions of acetylcholine as the primary excitatory neurotransmitter. The administration of the muscarinic cholinergic receptor antagonist atropine to healthy subjects resulted in difficulty in initiating, and pain during, micturition (Cullumbine *et al.* 1955) and in some *in vitro* studies, atropine was shown to abolish electrically evoked contraction (Sjörgen *et al.* 1982; Sibley, 1984). There are other *in vitro* studies, however, which suggest a role for purinergic neurotransmission in normal voiding; Cowan & Daniel (1983), for example, demonstrated

This paper has online Supplemental material.

DOI: 10.1113/jphysiol.2008.162040

that atropine abolished only 50% of stimulated contractions, and others (e.g. Elmér *et al.* 1986; Hoyle *et al.* 1989; Luheshi & Zar, 1990) have shown atropine-resistant contractions, albeit comprising a smaller proportion of excitatory neurotransmission than is attributed to the actions of acetylcholine. The wide variation in reported contributions of purinergic neurotransmission to bladder voiding is partly explained by the methodological difficulty of evoking neural stimulation without also evoking potentially masking direct muscle stimulation (Hoyle *et al.* 1989). It is, however, generally agreed that purinergic neurotransmission is up-regulated in bladder dysfunction; Sjörgen *et al.* (1982) demonstrated, for example, that while atropine abolished contractions in preparations from normal bladders, preparations from pathological bladders exhibited contractions that were up to 50% atropine resistant.

It has been demonstrated that ATP, released from parasympathetic nerve terminals, binds to P2X receptors (Burnstock & Kennedy, 1985; Howson *et al.* 1988) on urinary bladder smooth muscle cells (SMCs), producing an excitatory junction potential (EJP) that triggers the opening of L-type Ca^{2+} channels and the subsequent initiation of an action potential (Hoyle & Burnstock, 1985; Howson *et al.* 1988). Heppner *et al.* (2005) recently identified purinergic focal Ca^{2+} transients, corresponding to the influx of Ca^{2+} through P2X receptors upon ATP binding in rat urinary bladder smooth muscle.

In summary, although purines may not be the major excitatory neurotransmitters responsible for human bladder voiding, their up-regulated role in pathological states and with ageing makes purinergic neurotransmission a key area of study. The aims of the present study are to: (i) use simultaneous electrophysiological recording of membrane potential and high-speed imaging of Ca^{2+} fluorescence to determine whether a relationship exists between spontaneous purinergic Ca^{2+} transients and spontaneous depolarizations in mouse urinary bladder smooth muscle, and (ii) to characterize spontaneous depolarizations and, in particular, to determine the mechanisms underlying their generation.

Methods

General

Mice of the C57BL/6 strain, of either sex, weighing 18–30 g, were killed by head concussion followed by cervical dislocation. Efforts were made to minimize the number of animals used and their suffering; all experiments were carried out in accordance with the UK Animals (Scientific Procedures) Act 1986 and European Communities Council Directive 86/09/EEC.

The urinary bladder was removed and its ventral wall was opened longitudinally from the bladder neck (posterior) to the top of the dome (anterior). The urothelium was removed by careful dissection using iris scissors; care was taken not to stretch or damage the underlying detrusor muscle. Tissue strips, which contained a few bundles of smooth muscle, 6–8 mm long and 1–2 mm wide, were cut along the craniocaudal axis of the dorsal surface of the detrusor. Strips were pinned out on a Sylgard (Dow Corning Corporation, Midland, MI, USA)-lined plate at the bottom of a shallow chamber (volume, approximately 1 ml), which was mounted on the stage of an upright microscope. Preparations were superfused with warmed (35°C) physiological saline solution (PSS) (composition, mM: NaCl, 120; KCl, 5.9; $MgCl_2$, 1.2; $CaCl_2$ 2.5; $NaHCO_3$, 15.5; NaH_2PO_4, 1.2 and glucose, 11.5; gassed with 95% O_2 and 5% CO_2) at a constant flow rate (100 ml h^{-1}), maintaining a pH of 7.2–7.3 (Hashitani & Brading, 2003). Preparations, when pinned, were allowed to equilibrate (i.e. to accommodate under tension) for at least 30 min before electrophysiological recording or Ca^{2+} imaging.

Electrophysiological recordings

Individual bladder smooth muscle cells in muscle bundles were impaled with glass capillary microelectrodes, filled with 0.5 M KCl (tip resistance, 100–300 MΩ). Membrane potential changes were recorded using a high input impedance amplifier (Axoclamp-2B, Axon Instruments, Inc., Sunnyvale, CA, USA) and displayed on a digital oscilloscope (DSO 1602, Gould, Ilford, UK). Membrane potential changes were digitized using PowerLab/4SP (ADInstruments, Chalgrove, UK) at 4 kHz and stored on computer for later analysis.

Recordings were made from a minimum of six cells, for at least 5 min each, in the absence of drugs ('control' measurements). One long, continuous recording was then made, which included a control period (typically 10 min), and then a period (up to 1 h) in the presence of the drug. Recordings were subsequently made from a further six cells (minimum), for at least 5 min each. Subsequent analysis of the effect of the superfused reagents compared the median frequency for all cells recorded in the control period with the median frequency of events in the presence of the reagent, in a paired comparison.

Ca^{2+} imaging and analysis

Each detrusor strip was exposed to 10 μM Oregon Green 488 BAPTA-1 AM (Invitrogen, Paisley, UK) in 1% DMSO–0.2% Pluronic F-127 (Sigma-Aldrich, St Louis, MO, USA) in physiological salt solution (PSS) for 70 min at 36°C. The tissue was rinsed in PSS, bubbled with 95% O_2–5% CO_2, for at least 10 min. Tissues were pinned flat,

serosal side up, in a Sylgard-lined organ bath, and mounted on the stage of an upright confocal microscope (Leica SP2 upright confocal microscope; Leica Microsystems, Milton Keynes, UK).

A series of 200 frames was captured at 13.5 Hz to generate one image set. Such sets were acquired once every minute. Ten sets were generated for each region of the preparation, with at least three regions sampled per drug treatment and/or preparation.

Microelectrodes used for simultaneous confocal recordings (tip resistances of 200–300 MΩ) were filled with a potassium salt of Oregon Green BAPTA-1 (100 μM in 0.5 M potassium acetate; weight 10 kDa; Invitrogen). The microelectrode tip (or part of it) was always within the field of view of the confocal image.

Image analysis was performed using plug-ins for ImageJ (http://rsb.info.nih.gov/ij/download.html) that were custom-written by Dr R. J. Amos to detect focal increases in fluorescence of the Ca^{2+} indicator. Data were exported to Excel (Microsoft, Redmond, WA, USA) for formatting and then to Spike 2 (Cambridge Electronic Design, Cambridge, UK) for analysis in conjunction with electrophysiological recordings.

Analysis of correlations between focal Ca^{2+} transients and spontaneous depolarizations

The peak amplitudes of focal Ca^{2+} transients and spontaneous depolarizations were calculated using a custom-written script for Spike 2. The threshold for determining focal Ca^{2+} transients varied between recordings in different SMCs. The threshold was adjusted until it provided specificity comparable to manual counting ($\Delta F/F$ range of 0.06–0.1).

Occasionally, > 1 coincident focal Ca^{2+} transient was observed within the impaled cell. In this instance, the amplitudes of spontaneous depolarizations and focal Ca^{2+} transients were not included in the subsequent analysis.

In order to estimate the time of initiation of focal Ca^{2+} transients, experiments were performed in which Ca^{2+} fluorescence was measured along the long axis of a SMC at a high acquisition rate (2 kHz) and the amplitudes and timing of focal Ca^{2+} transients were correlated with the membrane potential of the imaged cell, simultaneously measured using the previously described electrophysiological recording technique. Ca^{2+} fluorescence was measured in a 20 μm-wide window around each focal Ca^{2+} transient for the duration of each acquisition period (approx. 2 s) using ImageJ. Using a custom-written script for R (http://www.r-project.org) a curve was then fitted, comprising:

$y = C_o$ (the resting fluorescence), before the initiation of the focal Ca^{2+} transient (i.e. $t < t_o$), and

$y = C_o + A\left(e^{-k_1[t-t_o]} - e^{-k_2[t-t_o]}\right)$, thereafter (i.e. $t \geq t_o$). A is an arbitrary constant.

The time of initiation (t_o) was that giving the minimum residual sum of squares for this curve fit. This function arises from a simple model of Ca^{2+} influx through $P2X_1$ receptors, with Ca^{2+} then cleared by a first-order process (see Appendix).

Drug sources, preparation and application

Tetrodotoxin (Tocris, Bristol, UK), nifedipine (Bayer, Leverkusen, North Rhine-Westphalia, Germany) and atropine sulphate (VWR; Lutterworth, UK) were stored frozen (−20°C) at a concentration of 10 mM in DMSO. NF449 (at 1 mM; Tocris, Bristol, UK) and α-latrotoxin (at 300 nM; Sigma-Aldrich) were stored frozen in distilled water. Drugs were diluted to their final concentration in PSS and applied to the preparation by switching the superfusate from standard PSS.

Statistical analysis

The normality and homogeneity of variance was tested prior to further statistical analysis using Kolmogorov–Smirnov and Levene's tests, respectively (SPSS version 11, SPSS Inc., Chicago, IL, USA). Unless otherwise stated, statistical comparisons are Student's two-tailed paired t test. The term n, used in the presentation of statistical analyses throughout, refers to the number of animals used.

Results

Pharmacology of spontaneous depolarizations

Intracellular recording of smooth muscle cells in the mouse urinary bladder revealed both spontaneous depolarizations (sDeps) and spontaneous action potentials (sAPs), as previously described. sAPs can be distinguished from sDeps by their greater amplitude, the presence of an after-hyperpolarization or after-depolarization and their sensitivity to the voltage-dependent Ca^{2+} channel (VDCC) antagonist nifedipine (Meng *et al.* 2008).

In order to determine the mechanisms underlying the generation of sDeps, the contributions of purinergic and cholinergic neurotransmission were explored through the application of specific antagonists. The purinergic $P2X_1$ antagonist NF449 (10 μM) greatly reduced the frequency of sDeps. The frequency at which sDeps were detected was reduced from $8.0 \pm 3.6\ min^{-1}$ in control cells to $0.7 \pm 0.3\ min^{-1}$ following 1 h of superfusion with NF449 (post-NF449, $8.5 \pm 8.5\%$ of controls; $P < 0.01$, $n = 4$; Fig. 1*Aa* and *B*), with the amplitude of the remaining events reduced to $75 \pm 6\%$ of controls ($P < 0.05$, $n = 4$). Superfusion of the $P2X_1$-desensitizing agonist α,β-methylene ATP

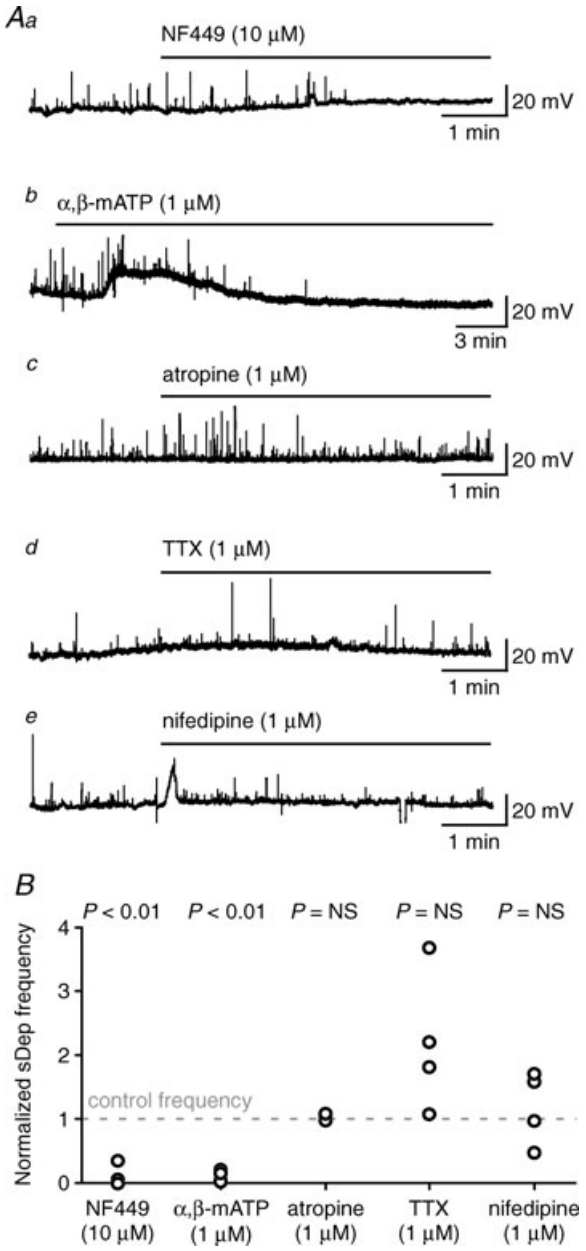

Figure 1. Spontaneous depolarizations (sDeps) are purinergic in origin

A, comparing the effects of the superfusion of the $P2X_1$ antagonist NF449 (10 μM) (*a*), the $P2X_1$-desensitizing agent α,β-methylene ATP (α,β-mATP; 1 μM) (*b*), the muscarinic acetylcholine receptor antagonist atropine (1 μM) (*c*), a blocker of Na^+ channels, tetrodotoxin (TTX, 1 μM) (*d*) and an antagonist of L-type Ca^{2+} channels, nifedipine (1 μM) (*e*) on the membrane potential of SMCs. Note the longer time-scale of *Ab*. A depolarization and increase in the sAP frequency induced by α,β-mATP (*Ab*) is initially noted (consistent with its action as an agonist), before the membrane potential returns towards its resting level and the sAPs decline in frequency (presumably as the receptors desensitize). *B*, a comparison of the frequency of sDeps for each drug application to normalized control frequencies, with paired *t* test statistical comparisons (see text for details).

(α,β-mATP; 1 μM) reduced the frequency with which sDeps were detected from $11.3 \pm 2.0\ min^{-1}$ in control cells to $1.4 \pm 0.6\ min^{-1}$ (post-α,β-mATP, $11.4 \pm 0.6\%$; $P < 0.01$, $n = 4$; Fig. 1*Ab* and *B*) with the amplitude of remaining sDeps reduced to $55 \pm 10\%$ of controls ($P < 0.05$, $n = 4$). In contrast to NF449 and α,β-mATP, the muscarinic acetylcholine receptor antagonist atropine (1 μM) did not affect the frequency of sDeps, which was $74 \pm 31\ min^{-1}$ in control cells and $76 \pm 31\ min^{-1}$ following 1 h application (post-atropine, $103.4 \pm 2.6\%$ of controls; P = not significant (NS), $n = 4$; Fig. 1*Ac* and *B*).

In the urinary bladder of the guinea pig, it has been reported that some large-amplitude sEJPs result from spontaneous nerve terminal action potentials (Bramich & Brading, 1996). In the present work in mouse urinary bladder, however, TTX (1 μM) did not abolish large-amplitude (> 10 mV) sDeps (range, control: 1.7–35.0 mV; TTX, following superfusion for 1 h: 1.4–31.2 mV, $n = 4$). TTX (1 μM) also did not affect the frequency of sDeps, which was $4.3 \pm 0.5\ min^{-1}$ in control cells, and $7.1 \pm 1.1\ min^{-1}$ following TTX (post-TTX, $166 \pm 55\%$ of controls; P = NS; Fig. 1*Ad* and *B*).

In order to determine whether blocking L-type Ca^{2+} channels affected the frequency at which sDeps were detected, the effect of nifedipine was assessed. Nifedipine (1 μM) did not affect the frequency of sDeps, which was $6.6 \pm 2.3\ min^{-1}$ in control cells, and $6.5 \pm 2.0\ min^{-1}$ following nifedipine superfusion for 1 h (post-nifedipine, $100 \pm 29\%$ of controls; P = NS; Fig. 1*Ae* and *B*).

In order to determine whether the ATP that initiates sDeps comes from nerves, experiments were performed in the presence of an extract of the black widow spider venom, α-latrotoxin (LTX), which increases the rate of spontaneous neurotransmitter release from nerve terminals. Superfusion of LTX (1 nM) for 10 min produced a $438 \pm 95\%$ increase in sDep frequency (to $35.3 \pm 8.3\ min^{-1}$) with respect to the control period ($9.3 \pm 2.6\ min^{-1}$) ($P < 0.05$, $n = 4$; Fig. 2*A*). The superfusion of atropine (1 μM), in addition to LTX (1 nM), produced a similarly large augmentation of sDeps, to $460 \pm 320\%$ ($63 \pm 13\ min^{-1}$) of control frequency ($13.8 \pm 2.8\ min^{-1}$) ($P < 0.05$, $n = 4$; Fig. 2*B*). By contrast, when LTX (1 nM) was superfused in addition to NF449 (10 μM) sDeps were completely abolished within 15 min ($n = 4$; Fig. 2*C*).

Pharmacology of spontaneous action potentials

Spontaneous action potentials (sAPs; of amplitude: 53.4 ± 2 mV) were observed in 38% of SMCs (i.e. 11 of 29, from $n = 4$) where they typically occurred at a low frequency ($0.77 \pm 0.20\ min^{-1}$, range: 0.2–2.6). Following superfusion of the $P2X_1$ antagonist NF449 (10 μM) for 1 h, sAPs were not observed in any SMC (i.e. 28 of 28, from

$n = 4$). To confirm that NF449 had no direct effect on L-type Ca^{2+} channels, SMC membrane properties were examined with a series of brief current injections. In control cells and those superfused with NF449 (10 μM) for 1 h, current injections $\geq +0.09$ nA stimulated active currents consistent with normal opening of L-type Ca^{2+} channels (see online Supplemental material, Fig. 1).

Superfusion of the $P2X_1$-desensitizing agent α,β-mATP (1 μM) reduced the number of SMCs in which sAPs were observed from 17 of 25 (from $n = 4$) in control cells to 4 of 20 following α,β-mATP superfusion (Fisher's exact test $P < 0.05$). The frequency of sAPs occurring in cells that had at least one sAP was reduced from 1.17 ± 0.44 min^{-1} in control cells to 0.141 ± 0.009 min^{-1} ($P < 0.05$, $n = 4$).

By contrast to the effects of NF449 and α,β-mATP, the muscarinic acetylcholine receptor antagonist atropine (1 μM) did not affect the frequency of sAPs, which was 0.54 ± 0.37 min^{-1} in control cells and 0.89 ± 0.58 min^{-1} following 1 h application (post-atropine, 126 ± 39% of controls; $P =$ NS, $n = 4$).

In order to determine the contribution of spontaneous activation of nerve branches or spontaneous nerve terminal action potentials to sAPs, the frequency of sAPs was compared following superfusion of TTX (1 μM). The frequency of sAPs was similar in control cells (0.52 ± 0.3 min^{-1}, range: 0.1–2.1; observed in 6 of 28 SMCs, from $n = 4$) to those superfused with TTX for 1 h (0.73 ± 0.40 min^{-1}, range: 0.1–2.1; observed in 7 of 28 SMCs, from $n = 4$) ($P =$ NS, Student's t test). The amplitudes of sAPs were unaffected by TTX superfusion (control: 50.1 ± 3.0 mV, post-TTX: 51.5 ± 2.0 mV; $P =$ NS, Student's t test).

In order to investigate whether sAPs result from nerve-released ATP, experiments were performed in the presence of LTX. Following the superfusion of LTX (1 nM) for 10 min, sAP frequency was increased to 930 ± 450% of control (i.e. 1.9 ± 0.5 min^{-1} to 11.0 ± 3.1 min^{-1}; $P < 0.05$, $n = 4$). sAPs were also increased in frequency following superfusion of LTX and atropine (1 μM) (600 ± 370% of control; from 0.4 ± 0.1 min^{-1} to 2.8 ± 1.8 min^{-1}; $P =$ NS, $n = 3$), but sAPs were abolished by LTX and NF449 (10 μM) (9 ± 5% of control; from 1.5 ± 0.6 min^{-1} to 0.1 min^{-1}; $P < 0.001$, $n = 4$).

The relationship between sDeps and sAPs

To determine whether sDeps might intermittently initiate sAPs, their kinetics were compared. Both sDeps and sAPs occurred with variable rising phases, with times-to-peak ranging from 5 to 89 ms for sDeps (median: 30 ms, no. of events = 4755, e.g. Fig. 3*A*) and 11–49 ms for sAPs (median: 19 ms, no. of events = 369, e.g. Fig. 3*B*). In order to test the hypothesis that the more prolonged rise times of sDeps indicate a lower peak current after ATP binding to $P2X_1$ receptors, the rising phases of both sDeps and sAPs were differentiated and compared. The differentiated rising phases of sDeps usually contained one peak, which varied in amplitude with a positively skewed distribution from 0.4 to 4.5 V s^{-1} (Fig. 3*A*). By contrast, the differentiated rising phase of sAPs always contained two determinable peaks and the broad amplitude frequency distribution (0.6–6.3 V s^{-1}) of the first peak is consistent with the highly variable time-to-peak of sAPs (Fig. 3*B*). Comparing the first peak of the differentiated rising phase of the depolarization revealed that the amplitude of the first derivative was much greater for sAPs (median: 2248 mV s^{-1}, range: 454–4913) than sDeps (median: 439 mV s^{-1}, range: 334–950) ($P < 0.0001$, $n = 12$, Wilcoxon signed rank test; Fig. 3*C*).

The L-type Ca^{2+} channel antagonist nifedipine (1 μM) abolished sAPs (Fig. 4*A*), and thus removed all depolarizations > 40 mV (Fig. 4*B*). We wanted to test the hypothesis that a subpopulation of large-amplitude depolarizations may trigger sAPs. If so, nifedipine should reveal a subpopulation of large-amplitude sDeps. No such subpopulation of large amplitude (e.g. 30–40 mV) sDeps was observed (e.g. data from a single, long-duration recording. Control, median amplitude: 8.8 mV, interquartile range: 6–13 mV; post-nifedipine: 8.1 mV, 6–14 mV; no. of sDeps was 996 and 355 for the

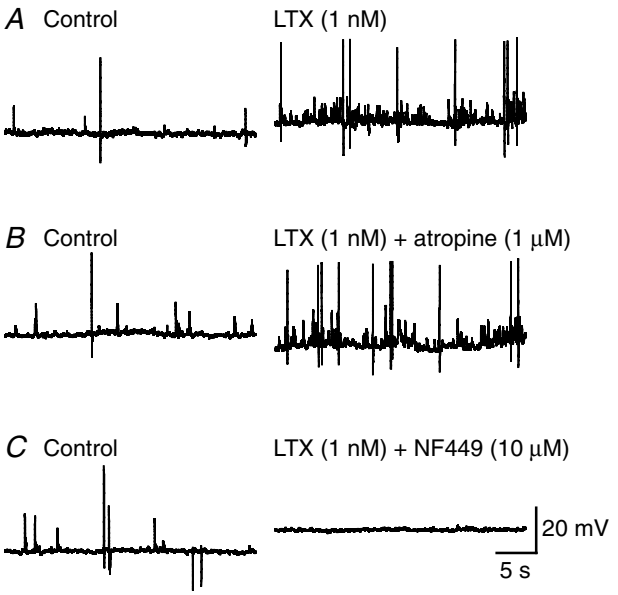

Figure 2. Spontaneous depolarizations are neurogenic
A, α-latrotoxin (LTX; 1 nM), which serves to increase the rate of spontaneous neurotransmitter release, caused an increase in the frequency of sDeps and spontaneous action potentials (sAPs). *B*, similarly, the superfusion of LTX and atropine (1 μM) produced a marked increase in the frequency of sDeps and sAPs. *C*, superfusion of LTX in combination with NF449 (10 μM), however, abolished all depolarizations. Data shown (i.e. control, then following 15 min drug superfusion) are excerpts from continuous recordings.

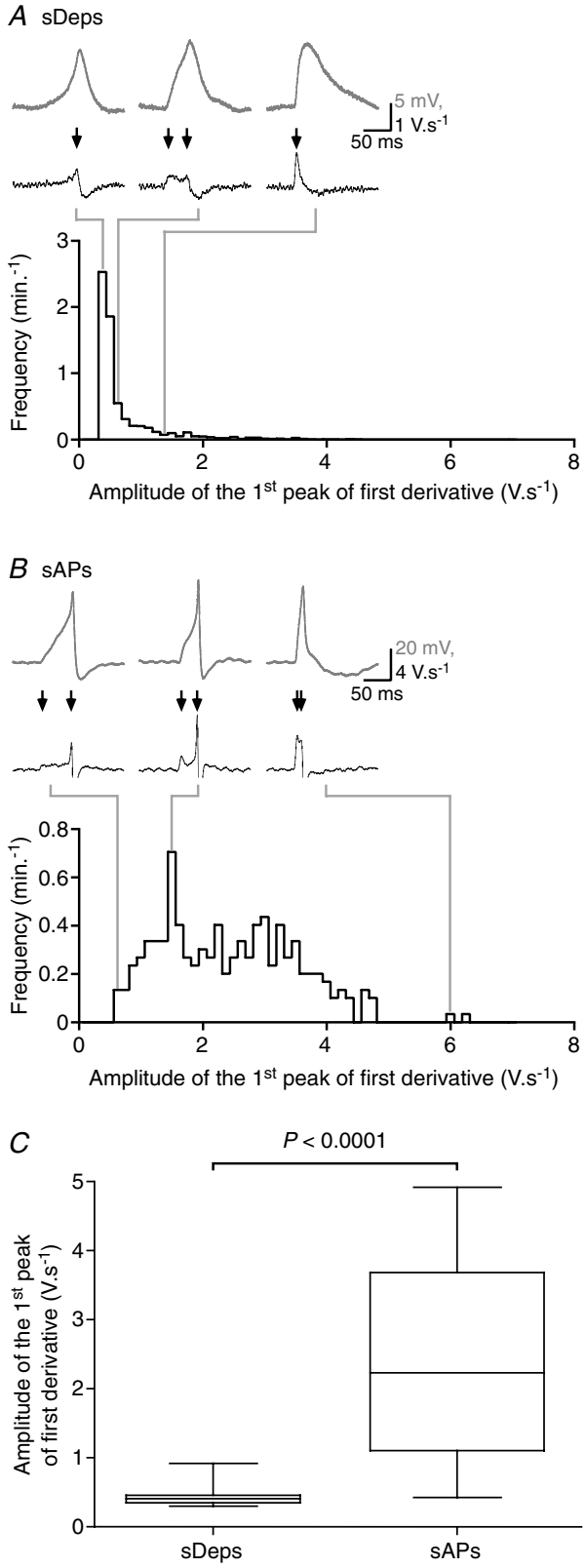

Figure 3. Peaks in the differentiated rising phases of sAPs are of, on average, larger amplitude than the differentiated peaks of sDeps

A, sDeps (grey trace) occurred with variable rising phases. When differentiated (black trace), peaks (arrows) occurred with a positively skewed amplitude distribution. *B*, sAPs (grey trace), which occurred with similarly varying waveforms as sDeps, reveal two peaks (arrows) when differentiated (black trace); the amplitude of the first peak of which has a broad amplitude distribution. Data shown for *A* and *B* are from a single, long-duration recording. Bin sizes for the amplitude distributions of first derivatives are 0.125 V s^{-1}. Note that the scale bars associated with the raw data of *A* and *B* are of differing magnitudes, and that the differentiated sAPs (*B*) are truncated at –1 V s^{-1}. *C*, the median amplitude of the first peak of the differentiated sAP is greater than the amplitude of the differentiated sDep. Data are median, quartiles and range ($n = 12$). See text for details of statistical comparison.

control and post-nifedipine periods, respectively. P = NS, Mann–Whitney U test) (Fig. 4*B*).

However, the peak inward current through $P2X_1$ receptors might provide a more sensitive measure of transmitter release than the amplitude of sDeps. To assess the inward current through $P2X_1$ receptors, the differentiated rising phases of only sDeps, pre- and post-superfusion with nifedipine (1 μM), were compared. The amplitude of the first derivative of the sDep increased from 237 mV s^{-1} in control cells (median amplitude; range: 182–359) to 268 mV s^{-1} (range: 196–422) following nifedipine superfusion (i.e. to 113 ± 3% of controls; Student's one-tailed paired t test, $P < 0.05$, $n = 4$) (data shown for one experiment, Fig. 4*C*). In control cells of these experiments, sAPs represented 12% (range: 3–21) of all depolarizations.

The relationship between spontaneous depolarizations and focal Ca^{2+} transients

Loading detrusor smooth muscle with the Ca^{2+} indicator Oregon Green BAPTA-1 AM revealed three types of spontaneous Ca^{2+} transient (whole-cell Ca^{2+} flashes, Ca^{2+} waves and focal Ca^{2+} transients), as reported by Meng *et al.* (2008). Simultaneous electrophysiology and confocal imaging of Ca^{2+} indicator fluorescence was used to determine the relationship between spontaneous depolarizations (sDeps) of the membrane potential of SMCs, with spontaneous focal, transient increases in fluorescence. Focal Ca^{2+} transients (Fig. 5*A*) were coincident with sDeps (Fig. 5*B* and *C*).

The relationship between these two events was explored with higher temporal resolution (2 kHz), by correlating line-scans taken along the long axis of a SMC (Fig. 6*A*), with a simultaneous measure of the membrane potential, recorded with an intracellular electrode impaled in the imaged cell. A focal Ca^{2+} transient occurred as a local event along the x-axis of the line-scan (Fig. 6*B*). A measure of the intensity of the Ca^{2+} fluorescence for this region revealed a rapid rise in $[Ca^{2+}]$ over a period of approximately 100 ms, and then a slow decline to baseline (Fig. 6*C*). For the same period of time and in the same cell, a sDep was observed that exhibits a rise-to-peak amplitude and time course of

decay that was much more rapid than the concurrent focal Ca^{2+} transient (459 ms; median half-decay time: 568 ms, range 329–921; $n = 3$). Expanding the scale (Fig. 6*D*), the rise in $[Ca^{2+}]$ starts approximately 8 ms after the initiation of the sDep. The latency of rise in $[Ca^{2+}]$ relative to the initiation of a sDep was calculated for 12 events occurring in preparations from three animals. The median latency was 10.4 ms (range: 4.3–25.8 ms).

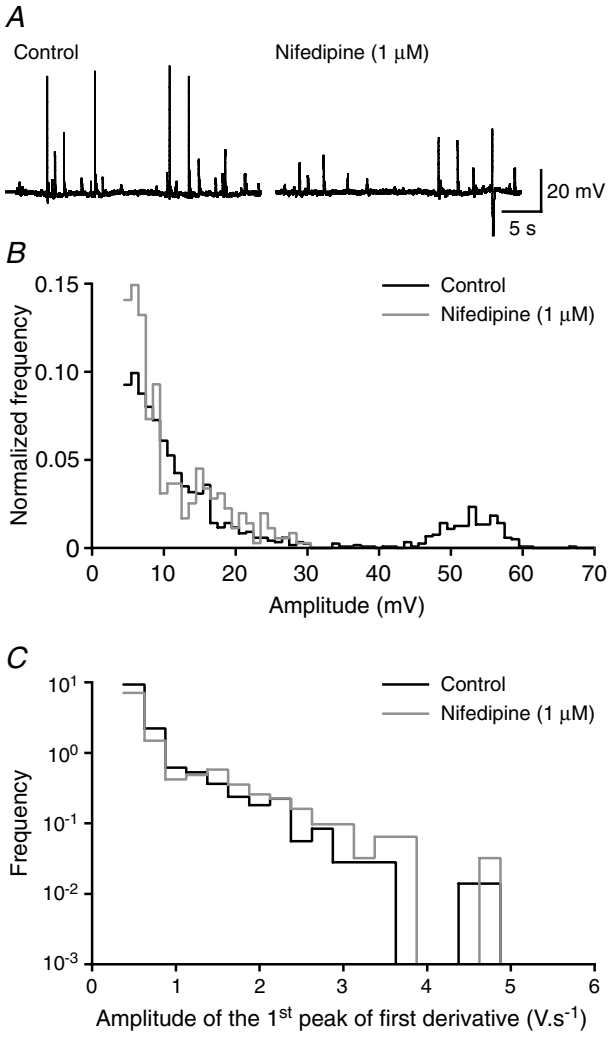

Figure 4. Blocking sAPs, through the application of nifedipine, reveals a subpopulation of sDeps with an especially rapid rising phase

A, superfusion of nifedipine (1 μM; 15 min superfusion) abolished sAPs in murine detrusor smooth muscle. A spontaneous depolarization with a following prolonged hyperpolarization was incidentally observed in the trace in the presence of nifedipine; such events were also occasionally observed in control cells (not shown) and have not been further characterized. Data shown are from a continuous recording. *B*, the amplitude frequency distribution post-nifedipine does not reveal a subpopulation of large amplitude sDeps; only the loss of depolarizations > 40 mV in amplitude. The threshold for detecting sEJPs was 2 mV. *C*, differentiated rising phases of sDeps reveal an increase in the frequency of larger amplitude events following nifedipine (1 μM) superfusion, compared to a control period.

The model fit to the Ca^{2+} signal (e.g. Fig. 6*D*) is based on an exponentially declining calcium influx, which is then removed by a first-order process. The change in membrane potential is proportional to the number of P2X receptors open (i.e. the conductance change) and

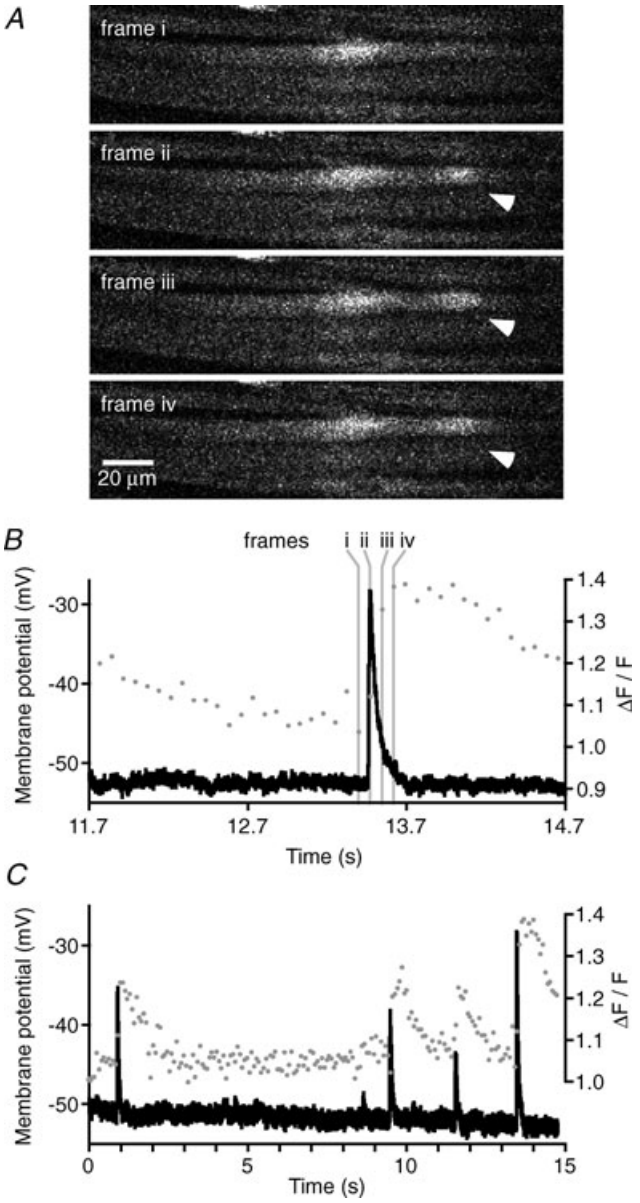

Figure 5. Spontaneous focal Ca^{2+} transients are coincident with spontaneous depolarizations (sDeps) in mouse urinary bladder smooth muscle

A, a region of a smooth muscle cell (SMC) in a mouse isolated urinary bladder (loaded with the Ca^{2+} indicator Oregon Green 488 BAPTA-1 AM) during an intracellular recording. Images, acquired at 13.5 Hz, are 4 consecutive frames of a 200 frame series. A spontaneous focal Ca^{2+} transient occurred on frame ii (arrowhead). *B*, intracellular recording of a period that includes the same four frames that compose *A*, showing simultaneous recordings of membrane potential (black line) and whole-cell fluorescence (grey dots). *C*, simultaneous Ca^{2+} imaging and electrophysiology demonstrate the coincidence of focal Ca^{2+} transients and sDeps during a longer period.

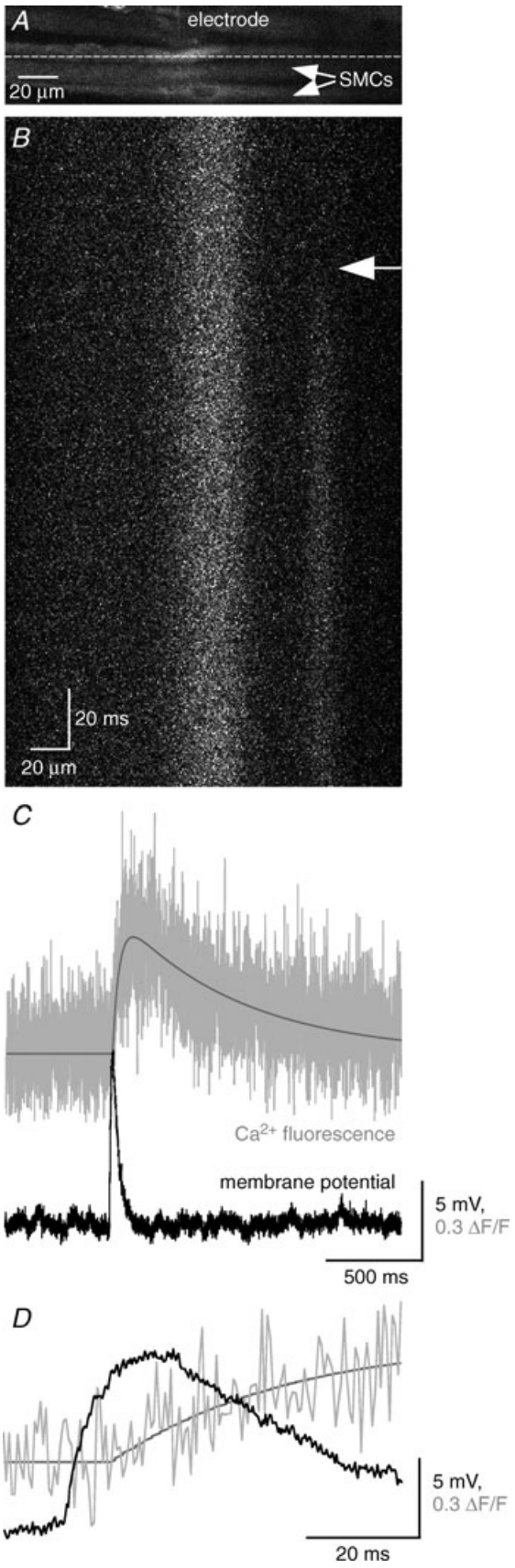

hence to the rate of Ca^{2+} influx (see Appendix). The sEJP fall time (median: 40 ms, interquartile range: 30–44 ms, calculated for 12 events which occurred in preparations from 3 animals) was similar to the estimate of the rate of Ca^{2+} influx, $1/k_2$ (median: 42 ms, 30–75 ms). There was no significant difference in the median time course of the sEJP and the modelled Ca^{2+} influx ($1/k_2$) ($P = \text{NS}$, Mann–Whitney U test), although these two measures were not correlated on a pair-wise basis (Spearman rank correlation, $\rho = -0.23$, and $P = \text{NS}$).

In addition to the temporal correlation, there was also a correlation in the amplitudes of focal Ca^{2+} transients and sDeps, both for large and small amplitude events (Pearson product moment correlation, $\rho > 0.41$ and $P < 0.05$ for each of $n = 3$ experiments; Fig. 7).

Whole-cell Ca^{2+} flashes and Ca^{2+} waves were also observed during simultaneous recordings, but both events occurred infrequently. Whole-cell Ca^{2+} flashes were observed to be concurrent with sAPs but Ca^{2+} waves did not correlate with any changes of the membrane potential of the impaled SMC.

In order to establish whether focal Ca^{2+} transients were associated with nerve terminal varicosities, parasympathetic neurones were visualized using the fluorescent dye, 3,3-diethyloxardicarbocyanine iodide ($DiOC_2(5)$; Yoshikami & Okun, 1984). Focal Ca^{2+} transients were observed close to nerve terminal varicosities (e.g. online Supplemental movie).

Discussion

Purinergic neurotransmission in the detrusor muscle of the human urinary bladder is up-regulated in pathological states (Palea *et al.* 1993) and with ageing (Yoshida *et al.* 2001). The mouse is an ideal model for the study of purinergic neurotransmission due to the relative ease with which transgenic animals can be produced (e.g. Vial & Evans, 2000) and because purinergic neuro-

Figure 6. Simultaneous Ca^{2+} imaging and electrophysiological measurement at a higher temporal resolution of imaging reveal the temporal relationship between focal Ca^{2+} transients and sDeps

A, a region of a smooth muscle cell (SMC) in a mouse isolated urinary bladder (loaded with the Ca^{2+} indicator Oregon Green 488 BAPTA-1 AM) during an intracellular recording. Line scans were taken along the long axis of an impaled SMC, the position of which is denoted by the dashed white line. *B,* line scan, acquired at 2 kHz, of the SMC (*A*) showing the occurrence of a focal Ca^{2+} transient (arrow). *C*, a measure of the Ca^{2+} fluorescence for a 20 μm region of the SMC in which the focal Ca^{2+} transient occurs (grey) compared to the membrane potential of the same cell for the same period of time (black). *D*, the occurrence of the focal Ca^{2+} transient (grey) and sDep (black) shown on an expanded time scale. The dark grey line of Ca^{2+} fluorescence (*C* and *D*) is a curve fitted using a custom-written script; see Methods for details.

transmission is a major component of detrusor excitation in this species (Holt *et al.* 1985; Meng *et al.* 2008). Thus, the aim of the current study was to characterize further spontaneous purinergic neurotransmission in the mouse urinary bladder, by first determining the origin of frequent 'spontaneous depolarizations' and spontaneous action potentials in smooth muscle cells (SMCs), and second to investigate their relationship to 'purinergic Ca^{2+} transients' (Heppner *et al.* 2005) identified in rat urinary bladder smooth muscle cells.

Spontaneous depolarizations are neurogenic, purinergic spontaneous excitatory junction potentials

ATP, released from nerve terminals, acts on $P2X_1$ receptors to cause frequent spontaneous depolarizations (sDeps) in the mouse urinary bladder. First, sDeps recorded using intracellular electrophysiology from SMCs were demonstrated to be purinergic in origin, consistent with the study of Meng *et al.* (2008). In the present study, sDeps were shown to be the result of ATP binding to $P2X_1$ receptors, as they were almost abolished by the specific $P2X_1$ receptor antagonist NF449 and the desensitizing agonist α,β-mATP (Fig. 1*B*). This conclusion is supported by the study of Vial & Evans (2000), in which ATP-induced inward currents were not present in bladder SMCs isolated from $P2X_1$ receptor-deficient mice. Also consistent with Meng *et al.* (2008) was the insensitivity of sDeps to atropine (1 μM; Fig. 1*B*). Second, the ATP that causes sDeps was shown to be released from nerve terminals. Following superfusion of α-latrotoxin (LTX; 1 nM), an agent which stimulates spontaneous neurotransmitter release (Ceccarelli & Hurlbut, 1980), the frequency of sDeps increased markedly (Fig. 2*A*). LTX-stimulated sDeps were abolished by NF449 (Fig. 2*C*) but were insensitive to atropine (Fig. 2*B*), suggesting that LTX did not stimulate acetylcholine release that, in turn, stimulated ATP release from, for example, SMCs.

The possibility that sDeps could be generated by spontaneous transient inward currents ('STICs') seems unlikely given that the time course of sDeps (49 ± 26 ms; Meng *et al.* 2008) is an order of magnitude briefer than stretch-induced STICs in isolated SMCs (approx. 500 ms; Ji *et al.* 2002). The detection of the sDeps before the onset of local Ca^{2+} transients (by about 10 ms), also argues against the Ca^{2+} transient activating a local ion conductance to generate a depolarization.

It should also be noted that there is unlikely to be any influence from urothelium-derived ATP (produced, for example, in response to stretch; Burnstock, 2001) as experiments were performed on muscle strips following careful removal of the urothelium, and recordings were made from the serosal surface.

The observations that sDeps were (i) increased in frequency by LTX, (ii) unaffected by TTX, and (iii) that their time course is very different to that of STICs recorded from isolated myocytes, imply that sDeps are the result of spontaneous neurotransmitter release from nerve terminals and are therefore spontaneous excitatory junction potentials (sEJPs).

Spontaneous action potentials (sAPs) are neurogenic and purinergic

Spontaneous action potentials (sAPs) were demonstrated to have a similar origin to sEJPs, i.e. nerve terminal-released ATP. sAPs, present in 38% of control cells sampled,

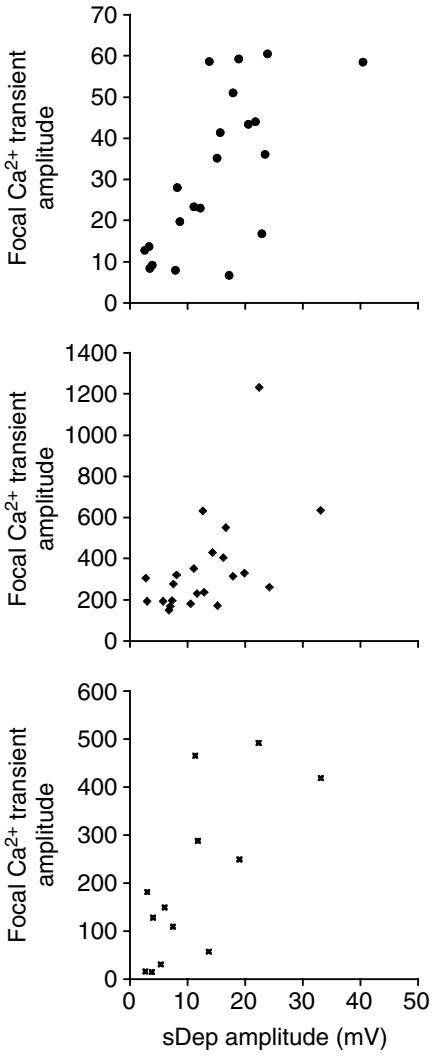

Figure 7. Focal Ca^{2+} transients and concurrent spontaneous depolarizations are correlated in amplitude
Correlations are shown for three recordings in which there were sufficient events to draw comparison of amplitudes.
Focal Ca^{2+} transient amplitude $= \frac{\Delta F}{F_o} \times \text{area}$, where ΔF is the change in fluorescence, F_o the resting fluorescence, and 'area' is the area over which the fluorescent signal is measured (in pixels) divided by 32; this is hence an arbitrary unit.

were not observed in any cells following the superfusion of NF449 and were almost abolished following $P2X_1$ receptor desensitization with α,β-mATP. By contrast, atropine (1 μM) did not affect the frequency of sAPs. These findings suggest that sAP frequency at rest is driven by the action of ATP on $P2X_1$ receptors rather than by acetylcholine.

sAP frequency was not influenced by spontaneous activation of nerve branches or spontaneous nerve terminal action potentials, as the frequency of sAPs was similar in control cells (0.52 min^{-1}; observed in 6 of 28 SMCs) to those superfused with TTX for 1 h (0.73 min^{-1}; observed in 7 of 28 SMCs). In order to investigate whether sAPs result from nerve terminal-released ATP, experiments were performed in the presence of LTX. Superfusion of LTX (1 nM) for 10 min increased sAP frequency to 930 ± 450% of control.

During the present series of experiments, the sAPs had a broad range of rise times with a prominent after-hyperpolarization, similar to the pacemaker-type sAPs previously described (Meng *et al.* 2008). Very few action potentials with only an after-depolarization (previously described as spike-type) were observed; such a difference might have arisen because the shallow angle of incidence of the electrode used in present work might select more superficial cells than the more vertical electrode approach used by Meng, Young and Brading (J. S. Young, personal observation). The shallow angle of electrode approach is necessary for the simultaneous Ca^{2+}-imaging experiments, so simultaneous recordings of a significant number of spike-type sAPs with Ca^{2+} measurements presents an unconquered technical hurdle.

The relationship between sEJPs and sAPs

It is likely that the EJP is the basis of urinary bladder smooth muscle action potentials; weak electrical stimulation evokes only an EJP, while stronger stimulation evokes an action potential (e.g. Creed *et al.* 1983; Brading & Mostwin, 1989).

Both sEJPs and sAPs occur with highly variable times-to-peak, ranging from 5 to 89 ms for sEJPs and 11–49 ms for sAPs. The peak amplitude of the first-time derivative of the rising phase is proportional to the peak current into the cell (Young *et al.* 2007*b*), thus in order to test the hypothesis that sAPs arise when the $P2X_1$ receptor current is high, the rising phases of both sEJPs and sAPs were differentiated for comparison. For a sAP, the differentiated rising phase revealed two peaks; the first attributed to the influx of cations through the P2X receptor, and second, the influx of Ca^{2+} ions through VDCCs (Fig. 3*B*). Thus comparing only the first peak of the differentiated rising phase of the depolarization revealed that the amplitude of the first derivative was much greater for sAPs than sEJPs. To further assess whether VDCC opening is correlated with the peak current into the cell through $P2X_1$ receptors, the differentiated rising phases of sEJPs were compared pre- and post-VDCC blockade. There was a significant increase in the amplitude of the first derivative following nifedipine (1 μM) superfusion. The magnitude of the increase in first-derivative amplitudes following nifedipine superfusion was, however, relatively small (13 ± 3%), but this is consistent with sAPs representing only a small proportion (12%) of the depolarizations observed.

An increase in the median first-derivative amplitude following VDCC blockade, taken together with a greater amplitude of the first derivative for sAPs than sDeps, suggests that sAPs are generated when a large-amplitude post-junctional response to spontaneous ATP release from nerve terminals depolarizes the smooth muscle membrane potential to the voltage threshold for L-type Ca^{2+} channels.

Focal Ca^{2+} transients are concurrent with sEJPs in mouse urinary bladder SMCs

Confocal imaging of Ca^{2+} fluorescence identified, for the first time, frequent, spontaneous focal Ca^{2+} transients in SMCs of the mouse urinary bladder (Fig. 5*A*). These events were similar in appearance and time course to purinergic Ca^{2+} transients of SMCs of mouse vas deferens (Brain *et al.* 2002), rat mesenteric arteries (Lamont & Wier, 2002) and the rat urinary bladder (referred to there as 'localized Ca^{2+} transients'; Heppner *et al.* 2005). To determine the relationship between the focal Ca^{2+} transients of the mouse urinary bladder and sEJPs, simultaneous intracellular electrophysiology and confocal imaging of Ca^{2+} fluorescence were performed. A temporal correlation between focal Ca^{2+} transients and sEJPs (Fig. 5*B* and *C*) was further examined at a high (2 kHz) resolution, which revealed a 10.4 ± 3.3 ms delay between the onset of a focal Ca^{2+} transient and a sEJP recorded from the same SMC (Fig. 6*D*). This delay is of similar magnitude to the delay at neuroeffector junctions of the mouse vas deferens (6 ms; Brain *et al.* 2002) and rat urinary bladder (12–16 ms; Heppner *et al.* 2005). Binding of ATP to $P2X_1$ receptors generates an influx of Na^+ ions and Ca^{2+} ions (Isenberg *et al.* 1992; Evans *et al.* 1996), but it is unlikely that these movements are genuinely separated by 10 ms in SMCs of the mouse urinary bladder. During the first few milliseconds, the Ca^{2+} entering the cell is located close to the P2X receptors; the high local Ca^{2+} concentration saturates the high-affinity Ca^{2+} indicator so that the mean fluorescent signal underestimates the mean Ca^{2+} concentration during the initial period of Ca^{2+} entry. This non-linearity might account for at least part of the estimated delay. High endogenous Ca^{2+} buffering close to the plasma membrane would also induce such an effect. It is also possible that calcium-induced calcium release (CICR) augments the Ca^{2+} that enters the cell

through the $P2X_1$ receptor upon ATP binding, causing the delay between the onsets of the sEJP and the focal Ca^{2+} transient. CICR has been demonstrated to contribute to purinergic Ca^{2+} transients in SMCs of the guinea-pig urinary bladder (Imaizumi *et al.* 1998; Hashitani *et al.* 2000) and mouse vas deferens (Brain *et al.* 2003), but plays little role in SMCs of the mesenteric arteries (Lamont & Wier, 2002) or urinary bladder (Heppner *et al.* 2005) of rat. The potential contribution by CICR to focal Ca^{2+} transients in mouse urinary bladder SMCs awaits further experiments to inhibit CICR.

Focal Ca^{2+} transients correlate in amplitude with concurrent sEJPs

In addition to temporal coupling, focal Ca^{2+} transients and sEJPs were also correlated in amplitude throughout the amplitude range (Fig. 7). It has been suggested that spontaneous focal transients only arise from the release of the contents of a subpopulation of synaptic vesicles, giant dense-cored vesicles (Blair *et al.* 2003), rather than all vesicle types. The correlation of focal Ca^{2+} transients with even low-amplitude sEJPs, also observed in another smooth muscle organ, the mouse vas deferens (Young *et al.* 2007*a*), argues against this hypothesis. As argued elsewhere (Young *et al.* 2007*a*), an amplitude correlation of focal Ca^{2+} transients and sEJPs is contrary to the hypothesis that the variable amplitude of sEJPs results from the attenuation of depolarizations originating from distant release sites on neighbouring SMCs (Tomita, 1970; Purves, 1976). The hypothesis that the variable sEJP amplitudes represent the effects of ATP on only the impaled cell (Young *et al.* 2007*a*) is supported by the high input resistances of SMCs ($388 \pm 83\ M\Omega$) in this tissue (Meng *et al.* 2008).

The observation that sEJP fall time (40 ms) was similar to the estimate of the rate of Ca^{2+} influx, $1/k_2$ (42 ms) argues that the focal Ca^{2+} transients and sEJPs within a SMC are determined by a common mechanism – ion conductance through $P2X_1$ receptors.

As the focal Ca^{2+} transients described in the present study were shown to be correlated in timing and amplitude with sEJPs, themselves abolished by the $P2X_1$ receptor antagonist NF449, it is likely that the focal Ca^{2+} transients are purinergic in origin. It is unlikely that the focal Ca^{2+} transients observed are sparks, as their time course (half-decay time, 568 ms) was similar to purinergic Ca^{2+} transients of rat urinary bladder smooth muscle (112 ± 9 ms; Heppner *et al.* 2005) and much greater than that of sparks in urinary bladder smooth muscle (34 ± 5 ms, Heppner *et al.* 2005), mouse urinary bladder myocytes (69 ± 9 ms, Fritz *et al.* 2007) or vascular smooth muscle (range from 27 ms, Mironneau *et al.* 1996; to 61 ms, Jaggar *et al.* 1998).

Whole-cell Ca^{2+} flashes correlate with sAPs

The present work confirms a correlation between whole-cell Ca^{2+} flashes and sAPs. The whole-cell Ca^{2+} flashes seem to represent the same type of event described as 'global Ca^{2+} flashes' in rat urinary bladder smooth muscle cells (Heppner *et al.* 2005), as they have similar spatial and temporal characteristics, are abolished when L-type Ca^{2+} channels are blocked, and decreased in frequency by P2X receptor inhibition or desensitization. In both cases these Ca^{2+} transients arise as a consequence of smooth muscle action potentials, commonly initiated by the action of ATP on P2X receptors.

Conclusions

We have characterized spontaneous purinergic neurotransmission in mouse urinary bladder smooth muscle, demonstrating frequent sEJPs and sAPs that result from nerve-released ATP binding to $P2X_1$ receptors, sAPs occurring when the $P2X_1$ current is sufficient to trigger L-type Ca^{2+} channel opening. sEJPs correlate in timing and amplitude with focal Ca^{2+} transients, suggesting that both events result from the same quanta of ATP binding to $P2X_1$ receptors and providing further evidence for a variable effective post-junctional response to ATP binding in electrically well-coupled smooth muscle. The present study demonstrates that sAPs and sEJPs are triggered by the stochastic release of ATP from parasympathetic nerve terminals.

Appendix

In SMCs of many organs the time course of the sEJP is determined by the rate at which $P2X_1$ channels inactivate (Åstrand *et al.* 1988). To model the Ca^{2+} kinetics in a focal Ca^{2+} transient, consider the $P2X_1$ receptors opening rapidly at $t = 0$ and then closing stochastically with a time constant of k_2. It is hypothesized that the $P2X_1$ receptor is the primary, or only, conductance for Ca^{2+} under these conditions. Hence, the Ca^{2+} influx also falls exponentially with a rate constant of k_2. Assume that Ca^{2+} is removed from the cells by a first-order process with a rate constant of k_1, then the change in Ca^{2+} concentration (C) is given by:

$$\frac{dC}{dt} = A_o e^{-k_2 t} - k_1 C \quad (1)$$

where A_o is a constant proportional to Ca^{2+} influx at $t = 0$. This has the solution (given the limiting case of $C = 0$ as t goes to infinity):

$$C = \frac{A_o}{(k_2 - k_1)}(e^{-k_1 t} - e^{-k_2 t}) \quad (2)$$

This can be checked by substitution.

Fitting this function to experimentally obtained line-scanning confocal microscopy data of smooth muscle Ca^{2+} during a focal Ca^{2+} transient allows k_2 to be calculated and compared with the known sEJP time constant.

The time at the peak Ca^{2+} concentration (t_{max}; found when $dC/dt = 0$) is:

$$t_{max} = \frac{\ln\left(\frac{k_1}{k_2}\right)}{(k_1 - k_2)}$$

The peak Ca^{2+} concentration (C_{max}) is hence found (by substituting t_{max} into eqn (2)) to be:

$$C_{max} = \frac{A_o}{(k_2 - k_1)}\left(\left(\frac{k_1}{k_2}\right)^{\frac{-k_1}{(k_1-k_2)}} - \left(\frac{k_1}{k_2}\right)^{\frac{-k_2}{(k_1-k_2)}}\right)$$

So, for constants k_1 and k_2, the peak Ca^{2+} concentration (C_{max}) is proportional to the number of $P2X_1$ receptors opened at $t = 0$ (as this is proportional to A_o).

References

Ambache N & Zar MA (1970). Non-cholinergic transmission by post-ganglionic motor neurones in the mammalian bladder. *J Physiol* **210**, 761–783.

Åstrand P, Brock JA & Cunnane TC (1988). Time course of transmitter action at the sympathetic neuroeffector junction in the rodent vascular and non-vascular smooth muscle. *J Physiol* **401**, 657–670.

Blair DH, Lin YQ & Bennett MR (2003). Differential sensitivity to calcium and osmotic pressure of fast and slow ATP currents at sympathetic varicosities in mouse vas deferens. *Auton Neurosci* **105**, 45–52.

Brading AF & Mostwin JL (1989). Electrical and mechanical responses of guinea-pig bladder muscle to nerve stimulation. *Br J Pharmacol* **98**, 1083–1090.

Brain KL, Cuprian AM, Williams DJ & Cunnane TC (2003). The sources and sequestration of Ca^{2+} contributing to neuroeffector Ca^{2+} transients in the mouse vas deferens. *J Physiol* **553**, 627–635.

Brain KL, Jackson VM, Trout SJ & Cunnane TC (2002). Intermittent ATP release from nerve terminals elicits focal smooth muscle Ca^{2+} transients in mouse vas deferens. *J Physiol* **541**, 849–862.

Bramich NJ & Brading AF (1996). Electrical properties of smooth muscle in the guinea-pig urinary bladder. *J Physiol* **492**, 185–198.

Burnstock G (2001). Purine-mediated signalling in pain and visceral perception. *Trends Pharmacol Sci* **22**, 182–188.

Burnstock G, Cocks T, Crowe R & Kasakov L (1978). Purinergic innervation of the guinea-pig urinary bladder. *Br J Pharmacol* **63**, 125–138.

Burnstock G & Kennedy C (1985). Is there a basis for distinguishing two types of P2-purinoceptor? *Gen Pharmacol* **16**, 433–440.

Ceccarelli B & Hurlbut WP (1980). Ca^{2+}-dependent recycling of synaptic vesicles at the frog neuromuscular junction. *J Cell Biol* **87**, 297–303.

Cowan WD & Daniel EE (1983). Human female bladder and its noncholinergic contractile function. *Can J Phys Pharm* **61**, 1236–1246.

Craggs MD & Stephenson JD (1985). Bladder electromyograms and function in monkeys after atropine. *Br J Urol* **57**, 341–345.

Creed KE, Ishikawa S & Ito Y (1983). Electrical and mechanical activity recorded from rabbit urinary bladder in response to nerve stimulation. *J Physiol* **338**, 149–164.

Cullumbine H, McKee WHE & Creasey NH (1955). The effects of atropine sulphate upon healthy male subjects. *Q J Exp Physiol Cogn Med Sci* **40**, 309–319.

Elmér M, Alm P & Kullendorff CM (1986). Innervation of the child urinary bladder. *Scand J Urol Nephrol* **20**, 267–273.

Evans RJ, Lewis C, Virginio C, Lundstrom K, Buell G, Surprenant A & North RA (1996). Ionic permeability of, and divalent cation effects on, two ATP-gated cation channels (P2X receptors) expressed in mammalian cells. *J Physiol* **497**, 413–422.

Fritz N, Morel JL, Jeyakumar LH, Fleischer S, Allen PD, Mironneau J & Macrez N (2007). RyR1-specific requirement for depolarization-induced Ca^{2+} sparks in urinary bladder smooth muscle. *J Cell Sci* **120**, 3784–3791.

Hashitani H & Brading AF (2003). Electrical properties of detrusor smooth muscles from the pig and human urinary bladder. *Br J Pharmacol* **140**, 146–158.

Hashitani H, Bramich NJ & Hirst GD (2000). Mechanisms of excitatory neuromuscular transmission in the guinea-pig urinary bladder. *J Physiol* **524**, 565–579.

Henderson VE & Roepke MH (1934). The role of acetylcholine in bladder contractile mechanisms and in parasympathetic ganglia. *J Pharm Exp Ther* **51**, 97–111.

Heppner TJ, Bonev AD & Nelson MT (2005). Elementary purinergic Ca^{2+} transients evoked by nerve stimulation in rat urinary bladder smooth muscle. *J Physiol* **564**, 201–212.

Holt SE, Cooper M & Wyllie JH (1985). Evidence for purinergic transmission in mouse bladder and for modulation of responses to electrical stimulation by 5-hydroxytryptamine. *Eur J Pharm* **116**, 105–111.

Howson W, Taylor EM, Parsons ME, Novell R, Wilczynska MA & Harris DT (1988). Synthesis and biological evaluation of ATP analogues acting at putative purinergic P2x-receptors (on the guinea pig bladder). *Eur J Med Chem* **23**, 433–439.

Hoyle CH & Burnstock G (1985). Atropine-resistant excitatory junction potentials in rabbit bladder are blocked by α,β-methylene ATP. *Eur J Pharmacol* **114**, 239–240.

Hoyle CH, Chapple C & Burnstock G (1989). Isolated human bladder: evidence for an adenine dinucleotide acting on P2X-purinoceptors and for purinergic transmission. *Eur J Pharmacol* **174**, 115–118.

Imaizumi Y, Torii Y, Ohi Y, Nagano N, Atsuki K, Yamamura H, Muraki K, Watanabe M & Bolton TB (1998). Ca^{2+} images and K^+ current during depolarization in smooth muscle cells of the guinea-pig vas deferens and urinary bladder. *J Physiol* **510**, 705–719.

Isenberg G, Ganitkevich VYa & Schneider P (1992). Ca^{2+} influx through voltage- and purinoceptor-operated channels estimated from $[Ca^{2+}]_c$ signals (myocytes from guinea-pig urinary bladder). *Adv Exp Med Biol* **311**, 369–371.

Jaggar JH, Stevenson AS & Nelson MT (1998). Voltage dependence of Ca^{2+} sparks in intact cerebral arteries. *Am J Physiol Cell Physiol* **274**, C1755–C1761.

Ji G, Barsotti RJ, Feldman ME & Kotlikoff MI (2002). Stretch-induced calcium release in smooth muscle. *J Gen Physiol* **119**, 533–544.

Krell RD, McCoy JL & Ridley PT (1981). Pharmacological characterization of the excitatory innervation to the guinea-pig urinary bladder in vitro: evidence for both cholinergic and non-adrenergic-non-cholinergic neurotransmission. *Br J Pharmacol* **74**, 15–22.

Lamont C & Wier WG (2002). Evoked and spontaneous purinergic junctional Ca^{2+} transients (jCaTs) in rat small arteries. *Circ Res* **91**, 454–456.

Liang SX, D'arbe M, Phillips WD & Lavidis NA (2000). Development of fast purinergic transmission in the mouse vas deferens. *Synapse* **37**, 283–291.

Luheshi GN & Zar MA (1990). Presence of non-cholinergic motor transmission in human isolated bladder. *J Pharm Pharmacol* **42**, 223–224.

Meng E, Young JS & Brading AF (2008). Spontaneous activity of mouse detrusor smooth muscle and the effects of the urothelium. *Neurourol Urodyn* **27**, 79–87.

Mironneau J, Arnaudeau S, Macrez-Lepretre N & Boittin FX (1996). Ca^{2+} sparks and Ca^{2+} waves activate different Ca^{2+}-dependent ion channels in single myocytes from rat portal vein. *Cell Calcium* **20**, 153–160.

Nergårdh A (1981). Neuromuscular transmission in the corpus-fundus of the urinary bladder. An in vitro study in the cat. *Scand J Urol Nephrol* **15**, 103–108.

Palea S, Artibani W, Ostardo E, Trist DG & Pietra C (1993). Evidence for purinergic neurotransmission in human urinary bladder affected by interstitial cystitis. *J Urol* **150**, 2007–2012.

Purves RD (1976). Current flow and potential in a three-dimensional syncytium. *J Theor Biol* **60**, 147–162.

Saito M, Gotoh M, Kato K & Kondo A (1991). Influence of aging on the rat urinary bladder function. *Urol Int* **47** (suppl. 1), 39–42.

Sibley GN (1984). A comparison of spontaneous and nerve-mediated activity in bladder muscle from man, pig and rabbit. *J Physiol* **354**, 431–443.

Sjörgen C, Andersson KE, Husted S, Mattiasson A & Moller-Madsen B (1982). Atropine resistance of transmurally stimulated isolated human bladder muscle. *J Urol* **128**, 1368–1371.

Tomita T (1970). Electrical properties of mammalian smooth muscle. In *Smooth Muscle*, ed. Bülbring E, Brading AF, Jones A & Tomita T, pp. 197–243. Edward Arnold, London.

Vial C & Evans RJ (2000). P2X receptor expression in mouse urinary bladder and the requirement of P2X1 receptors for functional P2X receptor responses in the mouse urinary bladder smooth muscle. *Br J Pharmacol* **131**, 1489–1495.

Yoshida M, Homma Y, Inadome A, Yono M, Seshita H, Miyamoto Y, Murakami S, Kawabe K & Ueda S (2001). Age-related changes in cholinergic and purinergic neurotransmission in human isolated bladder smooth muscles. *Exp Gerontol* **36**, 99–109.

Yoshikami D & Okun LM (1984). Staining of living presynaptic nerve terminals with selective fluorescent dyes. *Nature* **310**, 53–56.

Young JS, Brain KL & Cunnane TC (2007*a*). The origin of the skewed amplitude distribution of spontaneous excitatory junction potentials in poorly coupled smooth muscle cells. *Neuroscience* **145**, 153–161.

Young JS, Brain KL & Cunnane TC (2007*b*). Electrical and optical study of nerve impulse-evoked ATP-induced, P2X-receptor-mediated sympathetic neurotransmission at single smooth muscle cells in mouse isolated vas deferens. *Neuroscience* **148**, 82–91.

Acknowledgements

Dr R. J. Amos (formerly of Department of Pharmacology, University of Oxford, UK) for providing the custom-written plug-ins for image analysis. The Tri-Service General Hospital, Taipei, Taiwan, ROC, for a DPhil studentship, to E.M. The Wellcome Trust provided financial support (069768 to T.C.C.; 074128 Research Fellowship to K.L.B). We are grateful to Mr Ben Wild (College of Richard Collyer, West Sussex) for mathematical checking of the Appendix.

Supplemental material

Online supplemental material for this paper can be accessed at: http://jp.physoc.org/cgi/content/full/jphysiol.2008.162040/DC1